Energy 36 (2011) 3907–3916

Contents lists available at ScienceDirect

Energy

journal homepage: www.elsevier.com/locate/energy

Heat release and engine performance effects of soybean oil ethyl ester blending into diesel fuel

Andre Valente Bueno [a,*], José Antonio Velásquez [b,c], Luiz Fernando Milanez [d]

[a] Mechanical Engineering Department, Federal University of Ceara, CEP 60455-760, Fortaleza, CE, Brazil
[b] Mechanical Engineering Department, Pontifical Catholic University of Parana, CEP 80215-901, Curitiba, PR, Brazil
[c] Mechanical Engineering Department, Federal Technical University of Parana, CEP 80230-901, Curitiba, PR, Brazil
[d] Mechanical Engineering Faculty, University of Campinas, CEP 13083-970, Campinas, SP, Brazil

ARTICLE INFO

Article history:
Received 28 February 2010
Received in revised form
20 June 2010
Accepted 22 July 2010
Available online 2 September 2010

Keywords:
Diesel engine
Soybean ethyl ester biodiesel
Engine performance
Exergy analysis

ABSTRACT

The engine performance impact of soybean oil ethyl ester blending into diesel fuel was analyzed employing heat release analysis, in-cylinder exergy balances and dynamometric tests. Blends with concentrations of up to 30% of soybean oil ethyl ester in volume were used in steady-state experiments conducted in a high speed turbocharged direct injection engine. Modifications in fuel heat value, fuel–air equivalence ratio and combustion temperature were found to govern the impact resulting from the addition of biodiesel on engine performance. For the analyzed fuels, the 20% biodiesel blend presented the best results of brake thermal efficiency, while the 10% biodiesel blend presented the best results of brake power and *sfc* (specific fuel consumption). In relation to mineral diesel and in full load conditions, an average increase of 4.16% was observed in brake thermal efficiency with B20 blend. In the same conditions, an average gain of 1.15% in brake power and a reduction of 1.73% in *sfc* was observed with B10 blend.

1. Introduction

The esters of biological oils, also known as biodiesel, have been considered as promising renewable substitutes for mineral diesel fuel [1–3]. Biodiesel research to date has involved mostly methyl esters of vegetable oils in engines of different sizes and configurations, which were also operated under wide-ranging conditions of load and speed. Accordingly, the reported effects of biodiesel/diesel fuel blends on engine performance, combustion characteristics and emissions vary considerably.

Reductions in particulate matter, carbon monoxide and unburned hydrocarbon emissions can be achieved through the use of biodiesel. The substitution of diesel fuel by a B20 blend decreases the emission of particulate matter on average by 25% for engines meeting 2004 emissions standards [4] and by 10.1% for 1989 to 1994 model engines [5]. Engine characteristics have an even greater influence on nitrogen oxide emissions, with changes for the B20 blend ranging from +8 to −6% depending on the engine's technology, representing an average increase of 2% [5].

With regard to the brake thermal efficiency outcomes of biodiesel blending, reported data include slight elevations [6–15], inconclusive variations [16–20] and a slight decrease [21,22]. These results have been attributed to the following: reduction in friction power due to biodiesel lubricity [7,10], oxygen present in biodiesel [9,13], increase in combustion efficiency [6,7,12], improved combustion characteristics [8,23] and alterations in fuel vaporization and ignition processes [11].

In order to explain the behavior of the *sfc* (specific fuel consumption), some authors recognize a balance between the increased thermal efficiency and the fuel's reduced heating value resulting from the biodiesel blend. For such authors, the combination of these trends which provide the minimum *sfc* is achieved with B10 [6,10,11,14], B15 [12] or B20 [7,9,13] blends. Rakopoulos et al. [18] reported minimum fuel consumption with the B10 blend under moderate loads and with diesel fuel with the same engine operating under high loads, demonstrating that the impact of biodiesel blends on fuel consumption can also be regime-dependent. The break *sfc* reportedly decreased with biodiesel blends in studies which showed inconclusive variations or decreased thermal efficiency [21,22]. A third group of authors did not consider the effects on engine thermal efficiency, but investigated only alterations in break *sfc* resulting from the addition of biodiesel. In these works, dissimilar degrees of increase in *sfc* with biodiesel blending were reported and attributed directly to the differences in the heat

* Corresponding author. Tel.: +55 85 33669632; fax: +55 85 33669636.
E-mail address: bueno@ufc.br (A.V. Bueno).

0360-5442/$ – see front matter © 2010 Elsevier Ltd. All rights reserved.
doi:10.1016/j.energy.2010.07.030

values of the fuels [24–27] or to the combined effect of biodiesel's higher viscosity and lower calorific value [28].

In the present work, the effects of soybean oil ethyl ester/diesel blends on engine performance are studied through steady-state experiments conducted with a high speed turbocharged direct injection engine. Heat release analysis is applied in order to estimate the effects of biodiesel blending on the combustion process. Engine efficiency is accessed by means of two novel expressions developed for the exergy efficiencies of the combustion and expansion processes. These efficiencies are based on engine indicating data, providing information about the impact of biodiesel blends on the fractions of fuel exergy exchanged through work, destroyed by irreversibilities and lost with heat and mass transfers. The results obtained in the exergy analysis are employed to identify the causes of brake thermal efficiency, brake *sfc* and brake torque alterations measured in dynamometric bench tests.

2. Materials and methods

2.1. Tested fuels

Soybean oil ethyl ester is analyzed as a partial substitute for diesel fuel in concentrations of up to 30% by volume. The baseline fuel utilized here is a low sulphur (0.05%) diesel. Table 1 lists the relevant chemical, thermodynamic and physical properties of the test-fuels. Due to the presence of oxygen in its composition and a lower C/H ratio, biodiesel reduces the stoichiometric air–fuel mass ratio (a_{st}) and the chemical exergy of the fuel. The B20 blend, for instance, shows 10% higher fuel viscosity, 3.6% lower fuel exergy content and 2.6% lower amount of air necessary for stoichiometric combustion than diesel fuel. The viscosities of the diesel/biodiesel blends studied here were lower than would be predicted from a linear model, meeting the ASTM D-975 specification of a maximum of 4.1 $m^2 s^{-1}$ at 40 °C. A minor density increase also occurred with the addition of biodiesel, which was only 0.6% in the B20 blend.

2.2. Dynamometric bench tests

The experiments of this study were conducted at the Applied Thermodynamics Laboratory of the Pontifical Catholic University of Paraná. The tested engine was a direct injection, turbocharged, high speed diesel MWM 6.07T GMT-400, whose specifications are presented in Table 2. A ZÖLLNER ALFA-160 dynamometer and an AVL Puma 5 automated test bed system were used to control the engine's operation and identify its relevant parameters. Fuel consumption was determined with an AVL gravimetric fuel balance. The engine intake was connected to a surge tank, and the intake air volumetric flow rate was determined through a positive displacement-measuring device. The engine coolant and fuel temperatures were controlled with water-fed heat exchangers.

The engine brake *sfc* (specific fuel consumption) is given by measurements of brake power (P_b) and fuel mass flow rate (m_f):

Table 2
Engine specifications.

Configuration	4 Stroke, direct injection
Turbocharger control	Waste gate valve
Number of cylinders	6
Displacement [dm^3]	4.2
Bore [m]	0.093
Stroke [m]	0.103
Compression ratio	17.8:1
Valves per cylinder (intake/exhaust)	2/1
Intake valves close [deg after BDC]	32
Exhaust valve opens [deg before BDC]	55
Fuel injection pump	Bosch VE rotary distributor pump
Fuel injectors	5 Holes
Fuel injectors opening pressure (1st/2nd stage) [bar]	220/300
Piston crown shape	Re-entrant

$$sfc = \frac{\dot{m}_f}{P_b} \tag{1}$$

The engine brake thermal efficiency (η) constitutes a more fundamental parameter for comparisons of different fuels, taking into account the differences in the exergy values of these fuels:

$$\eta = \frac{P_b}{\dot{m}_f ex_f} \tag{2}$$

where ex_f is the specific flow exergy of the fuel studied here (see Section 2.5). Brake and indicated thermal efficiencies are utilized here to characterize the impact of the addition of biodiesel on engine efficiency. By combining Equations (1) and (2), it is possible to express the specific volumetric fuel consumption in terms of the fuel exergy and of the brake thermal efficiency:

$$sfc = \frac{1}{\eta \rho_f ex_f} \tag{3}$$

where ρ_f is the fuel density. The overall engine fuel–air equivalence ratio is considered through

$$\phi_{\text{overall}} = a_{\text{st}} \frac{\dot{m}_f}{\dot{m}_a} \tag{4}$$

Brake thermal efficiency data and performance maps obtained over the entire range of engine loads and speeds with baseline fuel and biodiesel blends are presented in contour graphs, which contain the brake mean effective pressure and the mean piston speed in the axes. The torque, in-cylinder pressure and fuel mass flow rate data utilized here were measured after 1 min of engine steady-state operation, with 200 rpm and 1/6 of maximum intervals of brake mean effective pressure between measurements. Overall fuel–air equivalence ratio, heat release and in-cylinder exergy analysis data are presented for full load conditions only. The accuracy of measurements and the uncertainty of calculated variables utilized here are shown in Table 3.

Table 1
Properties of diesel fuel, soybean ethyl ester (biodiesel) and its blends.

Fuel	% Biodiesel (Volume)	Empirical Formula	a_{st} $[m_f/m_{ar}]_{st}$	Density [kg/m^3]	Viscosity [m^2/s at 40 °C]	Ch. Exergy [MJ/kg]
Diesel	0%	$C_{10.80}H_{18.70}O_{0.00}$	14.60	850.0	2.60×10^{-6}	44.98 ± 0.15
B05	5%	$C_{11.03}H_{19.16}O_{0.05}$	14.51	851.3	2.66×10^{-6}	44.65 ± 0.15
B10	10%	$C_{11.27}H_{19.64}O_{0.11}$	14.41	852.6	2.72×10^{-6}	44.33 ± 0.15
B15	15%	$C_{11.53}H_{20.15}O_{0.16}$	14.33	853.9	2.79×10^{-6}	44.00 ± 0.14
B20	20%	$C_{11.80}H_{20.69}O_{0.22}$	14.22	855.2	2.86×10^{-6}	43.35 ± 0.14
B30	30%	$C_{12.38}H_{21.86}O_{0.35}$	14.04	857.8	3.09×10^{-6}	43.02 ± 0.14
Biodiesel	100%	$C_{19.75}H_{36.59}O_{2.00}$	12.77	876.0	4.57×10^{-6}	38.48 ± 0.12

Table 3
Accuracy of measurements and uncertainty of calculated variables.

Measurement	Full Scale Measurement Accuracy
Brake power	±0.32 kW
Fuel consumption (mass flow rate)	±192 g/h
Air consumption (volumetric flow rate)	±6 m^3/h
Indicated pressure	±0.67 bar
Calculated Variable	Calculated Variable Uncertainty
Fuel chemical exergy	±0.31%
Overall fuel–air equivalence ratio	±0.0107
Brake thermal efficiency	±0.0039
Specific volumetric fuel consumption	±1.84 ml/kWh
Gross indicated thermal efficiency (ΔEx_W)	±0.0048

2.3. Engine indicating experimental setup

A miniature piezoelectric pressure transducer AVL GM 12 D mounted flush above the piston bowl was used to measure the cylinder pressure. Thermal strain effects were prevented by adopting the test methods proposed by Randolph [29]. The transducer output was connected to a current to voltage converter, which provides in-cylinder pressure derivative signals. The differential pressure signal was averaged between 56 consecutive engine cycles and sampled with 0.5° crank angle resolution, using an AVL Indiset 317 indicating data acquisition system. Indicated pressure diagrams were obtained by numerical integration of the pressure derivative experimental data. The angular position of the top dead centre was determined dynamically by means of a capacitive sensor. The uncertainty shown in Table 3 for the indicated thermal efficiency ΔEx_W was calculated considering the combined accuracy of the system composed of the pressure transducer and the indicating data acquisition equipment [30].

2.4. Combustion diagnosis model

The processes taking place within the control volume shown in Fig. 1 were modeled according to the single-zone combustion model proposed by Krieger and Borman [31]. The injected fuel is considered to burn instantaneously as it enters the cylinder, and the working fluid is represented as a homogeneous mixture of combustion products passing through a sequence of equilibrium states. In-cylinder temperature (T) and instantaneous fuel–air equivalence ratio (ϕ) with the crank angle (θ) were determined from the following equations:

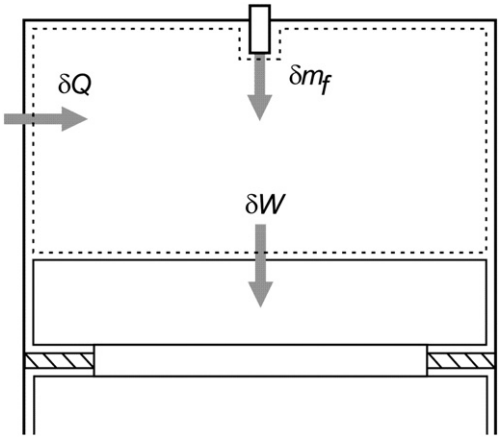

Fig. 1. Exergy and heat release analysis control volume.

$$\frac{dT}{d\theta} = \frac{\frac{1}{V}\frac{dV}{d\theta} + \left(\frac{1}{P} - \frac{1}{R}\frac{\partial R}{\partial P}\right)\frac{dP}{d\theta} - \left(\frac{1}{R}\frac{\partial R}{\partial \phi} + \frac{1}{a_{st}+\phi}\right)\frac{d\phi}{d\theta}}{\frac{1}{R}\frac{\partial R}{\partial T} + \frac{1}{T}} \tag{5}$$

$$\frac{d\phi}{d\theta} = \frac{\left(\frac{RT+A}{V}\right)\frac{dV}{d\theta} - \frac{RT}{PV}\frac{dQ}{d\theta} + \left(\frac{A}{P} - \frac{A}{R}\frac{\partial R}{\partial P} + \frac{du}{dP}\right) - \frac{dP}{d\theta}}{\frac{A}{R}\frac{\partial R}{\partial \phi} + \frac{\left(A + h_f - u\right)}{\phi + a_{st}}} \tag{6}$$

$$A = \frac{\frac{\partial u}{\partial T}}{\frac{1}{R}\cdot\frac{\partial R}{\partial T} + \frac{1}{T}} \tag{7}$$

where u is the specific internal energy of the working fluid, R is the gas constant of the working fluid, V is the cylinder volume, P is the cylinder pressure and h_f is the enthalpy of the fuel entering the combustion chamber. The thermodynamic properties of the working fluid and its partial derivatives related to T, P and φ were determined from a modified version of the PER and EQMD routines proposed by Olikara and Borman [32]. The modifications introduced into these routines allowed the working fluid entropy to be calculated and the composition of the air defined as the reference environment used in the exergy analysis to be taken into account. The heat transfer rate, $dQ/d\theta$, was estimated using the correlation proposed by Annand and Ma [33], and the heat transfer correlation adjusting parameters were set to obtain unitary combustion efficiencies. The combustion reaction extent is evaluated from:

$$\frac{dm_b}{d\theta} = \left(\frac{PV}{RT(\phi + a_{st})}\right)\frac{d\phi}{d\theta} \tag{8}$$

where $dm_b/d\theta$ is the apparent fuel mass burning rate. The crank angle periods required to a combustion reaction progress of 90% are computed in full load conditions, and averaged with 200 -rpm intervals of engine speed.

The numerical integration of Equations (5)–(8) provided the working fluid properties necessary for the exergy analysis discussed in the next section and the heat release analysis results presented in Fig. 3. These equations were solved during the closed valves period of the engine cycle, employing cylinder pressure and cylinder pressure derivative data obtained through the experimental procedures described in Section 2.3.

2.5. In-cylinder exergy balance and exergy efficiencies

The exergy balance for the control volume shown in Fig. 1 can be expressed in differential form as

$$\underbrace{\frac{dEx^{tm}}{d\theta}}_{1} + \underbrace{\frac{dEx^{ch}}{d\theta}}_{2} = \underbrace{\frac{dEx_Q}{d\theta}}_{3} - \underbrace{\frac{dEx_W}{d\theta}}_{4} + \underbrace{\frac{dEx_f}{d\theta}}_{5} - \underbrace{\frac{dI}{d\theta}}_{6} \tag{9}$$

where

$$\frac{dEx_f}{d\theta} = ex_f\frac{dm_f}{d\theta}$$
$$\frac{dEx_Q}{d\theta} = \left(1 - \frac{T^0}{T}\right)\frac{dQ}{d\theta}$$
$$\frac{dEx_W}{d\theta} = \left(P - P^0\right)\frac{dV}{d\theta}$$

The left-hand terms of the above equation represent the exergy variation rate of the system. These exergy components have opposite effects on the engine thermal efficiency. The thermomechanical exergy of the cylinder combustion gases can be

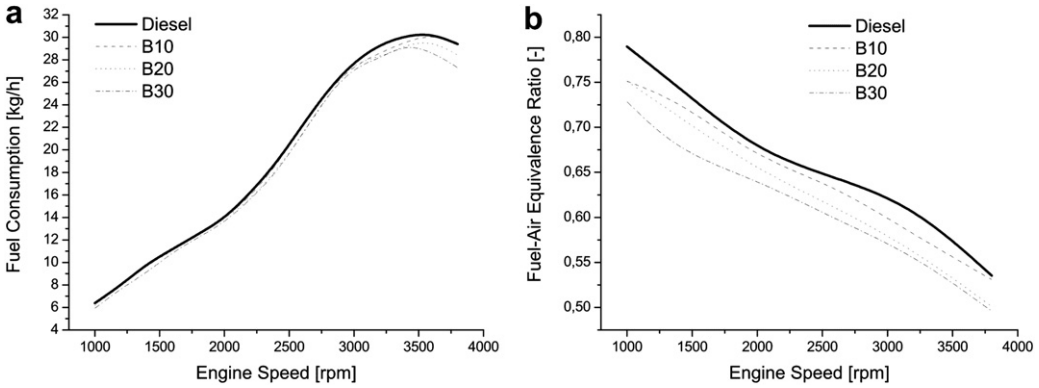

Fig. 2. Fuel consumption and fuel–air equivalence ratio under full load conditions.

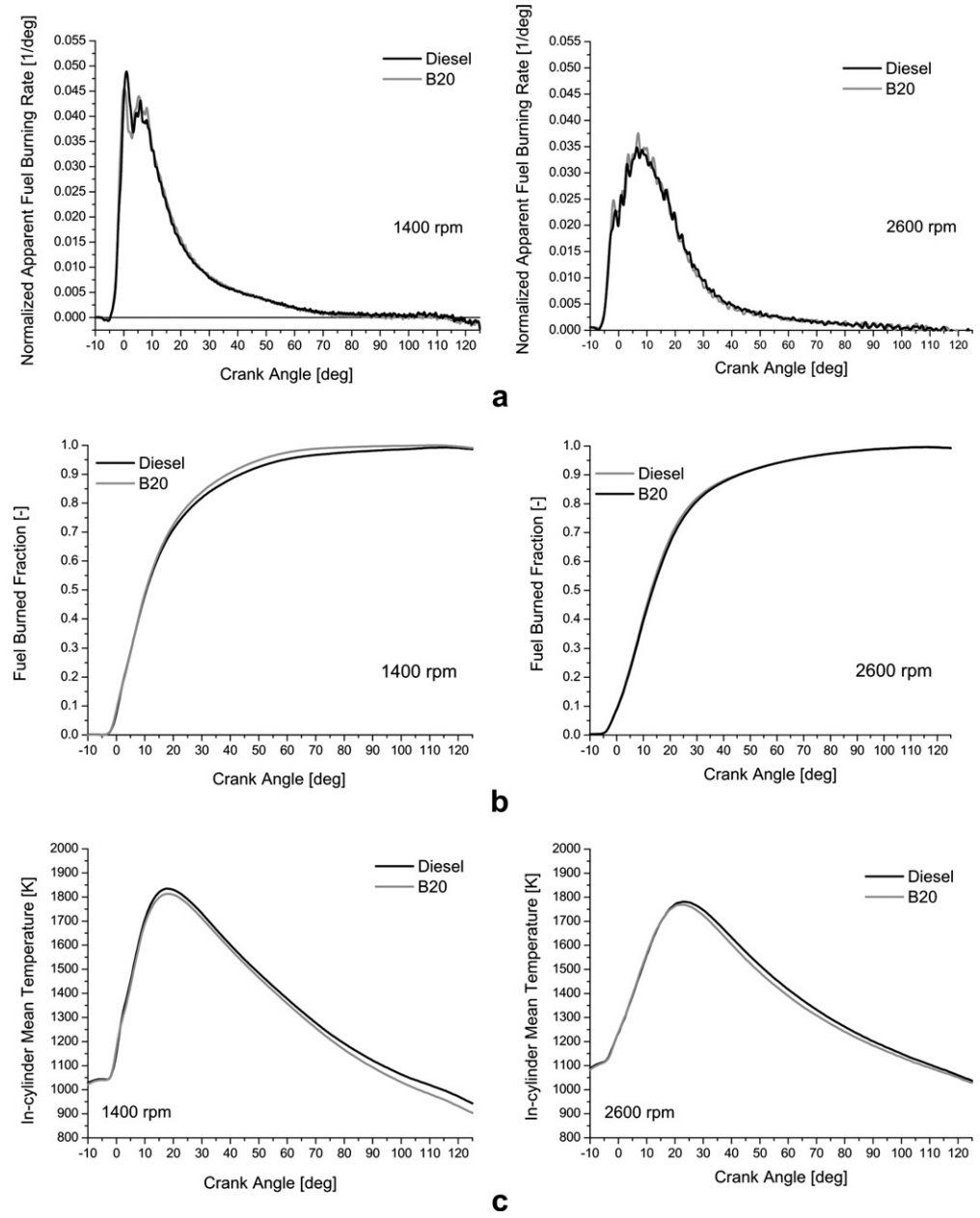

Fig. 3. Heat release analysis results obtained at full load regimes.

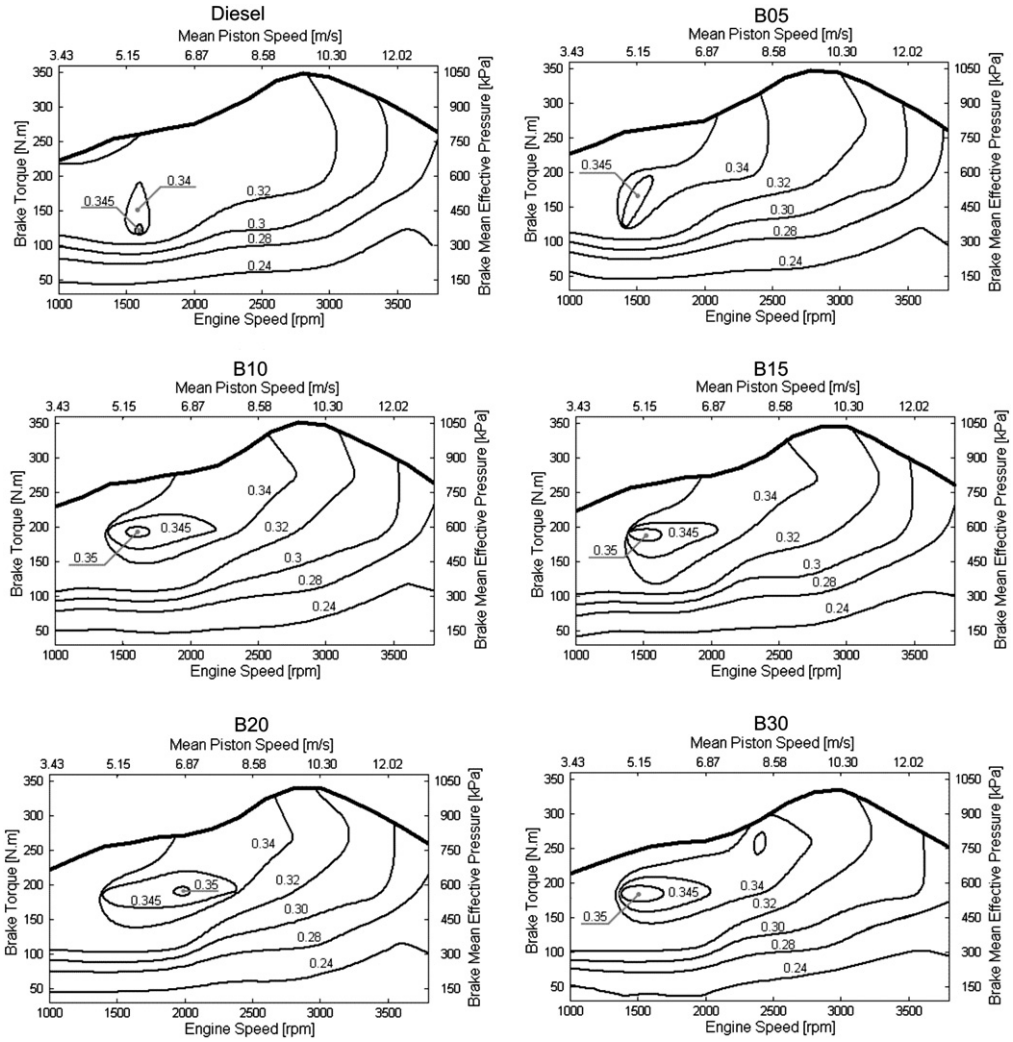

Fig. 4. Thermal efficiency maps for diesel fuel/biodiesel blends.

transferred through heat and work interactions occurring in the cylinder as well as in the exhaust system, while the chemical exergy of these gases cannot be converted into thermomechanical exergy or transferred through heat or work interactions inside the engine [34]. Consequently, it can be stated that the chemical exergy contained in the end-combustion gases represents a loss of exergy. The exergy transfers through the system boundaries associated to heat exchange (Ex_Q), indicated work (Ex_W), and fuel flow (Ex_f) are represented, respectively, in the third, fourth and fifth terms of the exergy balance equation. The destruction of exergy caused by irreversibilities associated with the fuel injection and combustion processes is considered in the sixth term of Equation (9), and its value was calculated from the Gouy–Stodola theorem.

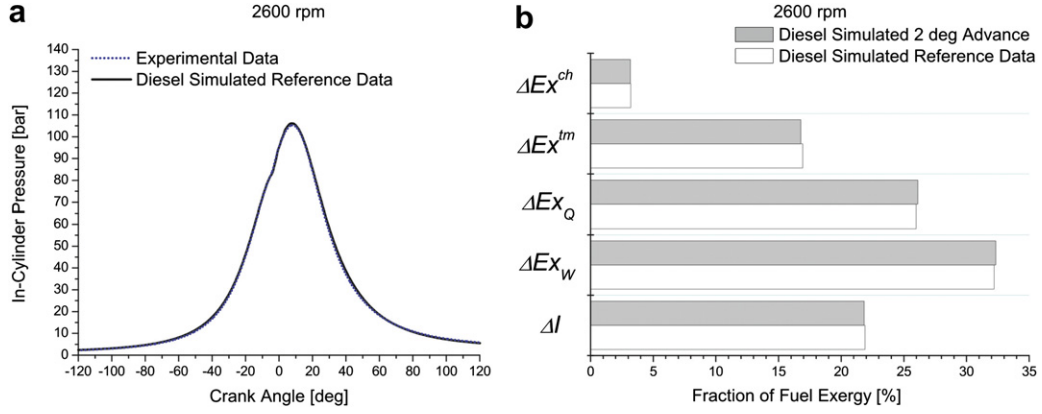

Fig. 5. Pressure and exergy balance results obtained for standard diesel combustion and 2° advanced mixing-controlled diesel combustion.

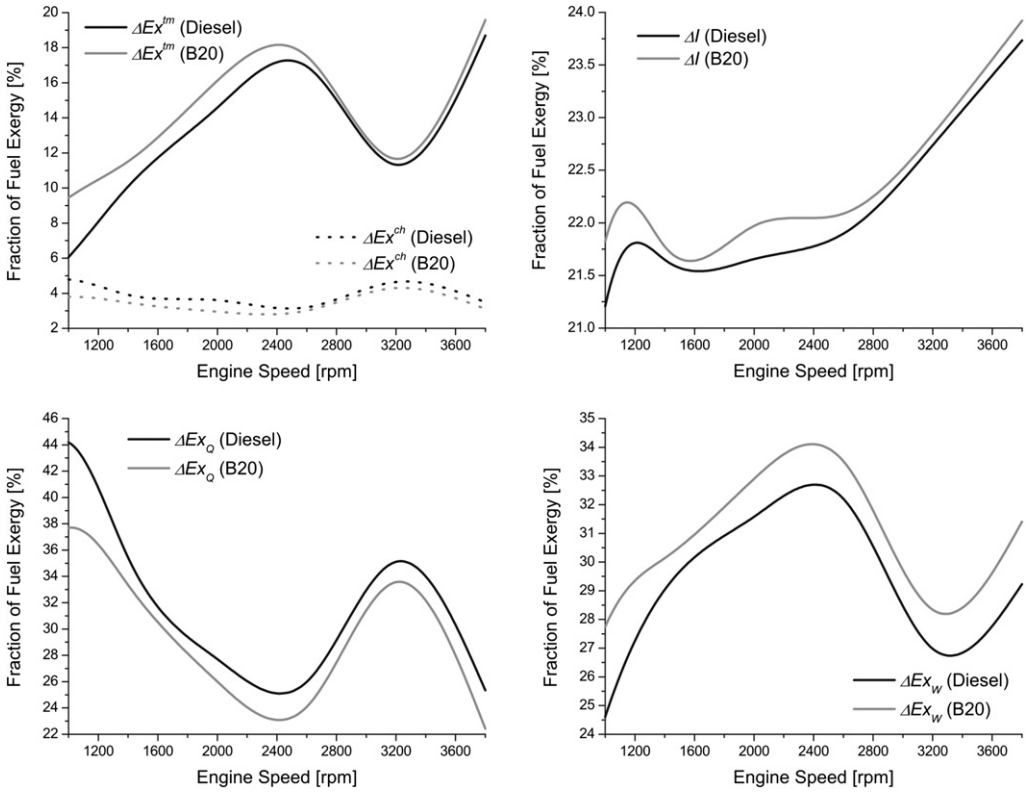

Fig. 6. In-cylinder exergy balance terms obtained for full load engine operation.

It is convenient to represent the terms of the exergy balance in the integral form, and normalized in relation to the exergy content of the injected fuel Ex_f :

$$\Delta Ex^{tm} + \Delta Ex^{ch} - \Delta Ex_Q + \Delta Ex_W + \Delta I = 1 \tag{10}$$

The first and the second terms of this equation represent the equivalent amounts of injected fuel exergy which remain in the form of thermomechanical (ΔEx_{tm}) and chemical (ΔEx_{ch}) exergies from combustion gases at the end of the closed part of the engine cycle. The term ΔI indicates the fraction of injected fuel exergy destroyed during combustion, while the terms—ΔEx_Q and ΔEx_W represent the fractions that have been transferred through heat and indicated work. Hence, as can be seen, the term ΔEx_W represents thermal efficiency derived from the gross indicated work. This term will, therefore, be used as a gross indicated thermal efficiency measure in Section 3.3. The exergy exchanged through heat transfer is considered a loss of exergy in this study, given that only a small part of it can be recovered through working fluid heating during admission and early compression, while most of it is destroyed by external irreversibilities.

The flow exergy of the fuels (ex_f) was evaluated through the following expression:

$$ex_f = h_f - T^0 s_f - \frac{\mu_f^0}{M_f} \tag{11}$$

In this equation μ_f^0 is the equivalent chemical potential of the fuel in ambient conditions, h_f is the specific fuel enthalpy, M_f is the fuel molecular weight and s_f is the specific entropy of the fuel. The enthalpies of formation of the diesel fuel and of the biodiesel were determined in function of experimentally obtained heats of combustion. The entropies of the fuels were estimated using an empirical expression [35], while the chemical potentials of the fuels were calculated in function of the chemical potentials of its combustion products:

$$\mu^0_{C_nH_mO_l} = n\mu^0_{CO_2} + \frac{m}{2}\mu^0_{H_2O} - \left(n + \frac{m}{4} - \frac{l}{2}\right)\mu^0_{O_2} \tag{12}$$

The reference environment adopted here corresponds to the air employed by Van Gerpen and Shapiro [36]. Further details regarding the working fluid model can be found in Ref. [14].

The normalized in-cylinder exergy balance can be re-written in the following form:

$$\Delta Ex_W = \eta_b \eta_{tm} \tag{13}$$

where

$$\eta_b = 1 - \Delta I - \Delta Ex^{ch} \tag{14}$$

$$\eta_{tm} = 1 - \frac{\Delta Ex^{tm} - \Delta Ex_Q}{1 - \Delta I - \Delta Ex^{ch}} \tag{15}$$

evidencing that the gross indicated thermal efficiency is composed of two other exergy efficiencies: a combustion exergy efficiency (η_b) that corresponds to the fraction of the fuel exergy that is converted into thermomechanical exergy of the working fluid through the combustion process; and a thermomechanical exergy transfer efficiency (η_{tm}) which is equivalent to the fraction of the thermomechanical exergy released by the combustion that is transferred through net indicated work. These exergy efficiencies and the cumulative terms of the in-cylinder exergy balance were computed in full load conditions only, and the averaged results presented in Section 3.3 were calculated with 200-rpm intervals of engine speed. Since the solution of the thermodynamic states of the working fluid considered here relies on experimental pressure diagrams, the exergy

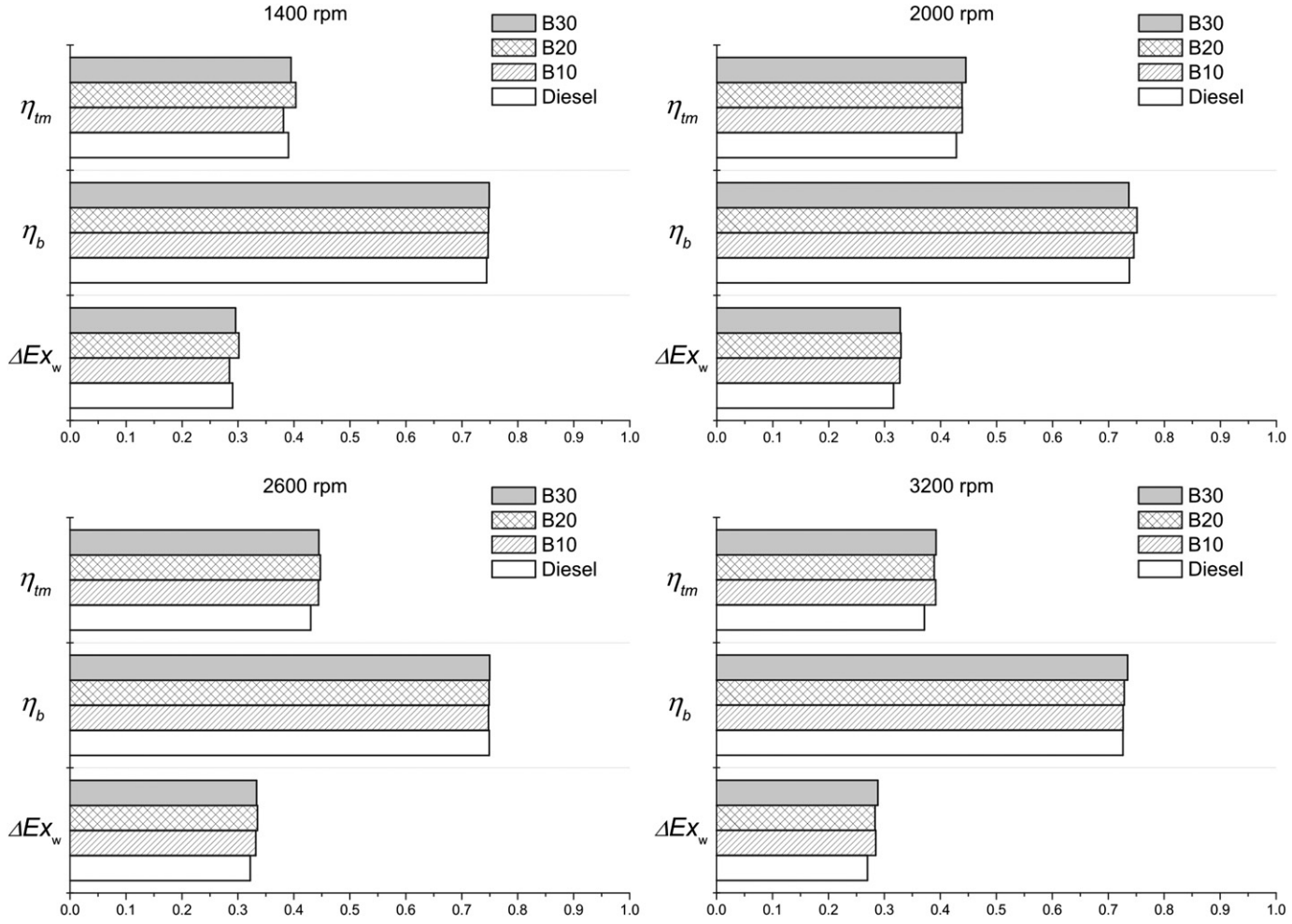

Fig. 7. Exergy efficiencies obtained for full load engine operation.

analysis data presented in Fig. 6 can be viewed as semi-experimental results, in a way similar to the well known heat release analysis.

3. Results and discussion

3.1. Combustion characteristics

Fig. 2a presents the fuel mass flow rate data obtained during full load operation with biodiesel blends and diesel fuel. Owing to the modifications introduced in the fuel's viscosity (see Table 1), the addition of biodiesel affects fuel pump lubrication and plunger/barrel blowby [19]. In the engine used in this study, the combination of these effects caused a reduction of the fuel mass flow rate as the concentration of biodiesel increased. However, this behavior was found to be significant only under moderate to high speeds. Since biodiesel (an oxygenated fuel) also has a lower stoichiometric air–fuel mass ratio (a_{st}), it would be reasonable to expect the engine to operate in overall leaner mixture conditions with the biodiesel blends [8]. The extent of the overall reduction in the fuel–air equivalence ratio is depicted in Fig. 2b.

Biodiesel viscosity also affects the fuel spray dynamics, increasing spray momentum, tip penetration and velocity [24,37–39]. Therefore, one can expect an important reduction in the local fuel–air equivalence ratio present in the fuel rich zones of the biodiesel spray combustion, as shown by Rakopoulos et al. [40]. The increase in the spray momentum promoted by biodiesel blending also improves the turbulent kinetic energy available in the fuel jet, which has a significant positive effect in the burning rate during the mixing-controlled combustion [41].

For the studied fuels, these modifications introduced in the fuel spray with biodiesel blending accelerated the processes of mixture preparation and burning, as can be seen in Fig. 3a and b. In full load conditions, the crank angle interval required to a combustion reaction progress of 90% presented an average reduction of 1.81 for B10 blend, 1.87 for B20 blend and 1.97 for B30 blend with relation to diesel fuel. These results are in accordance with those obtained by Tormos et al. [42], who explained the faster combustion obtained with neat biodiesel with an analogy between diesel spray and gas jet, concluding that neat biodiesel (B100) characteristic mixing time is always shorter for mixing-controlled combustion conditions. The lower in-cylinder mean temperatures observed in Fig. 3c for the B20 blend can be attributed to the previously commented reductions in the fuel heat value and injected mass caused by biodiesel addition to diesel fuel. As shown in Fig. 3a, the initial heat release rates of diesel and B20 were very well matched, which indicated that the biodiesel bulk modulus of compressibility, or speed of sound, does not affect the beginning of injection with the engine, rotary pump injection system and low biodiesel concentration fuel blends utilized here.

3.2. Engine brake thermal efficiency

Contour maps of engine brake thermal efficiency are shown in Fig. 4 [14]. For most engine operational conditions, biodiesel blending slightly increased the brake thermal efficiency. These results are qualitatively consistent with the effects of engine thermal efficiency enhancement reportedly achieved with neat

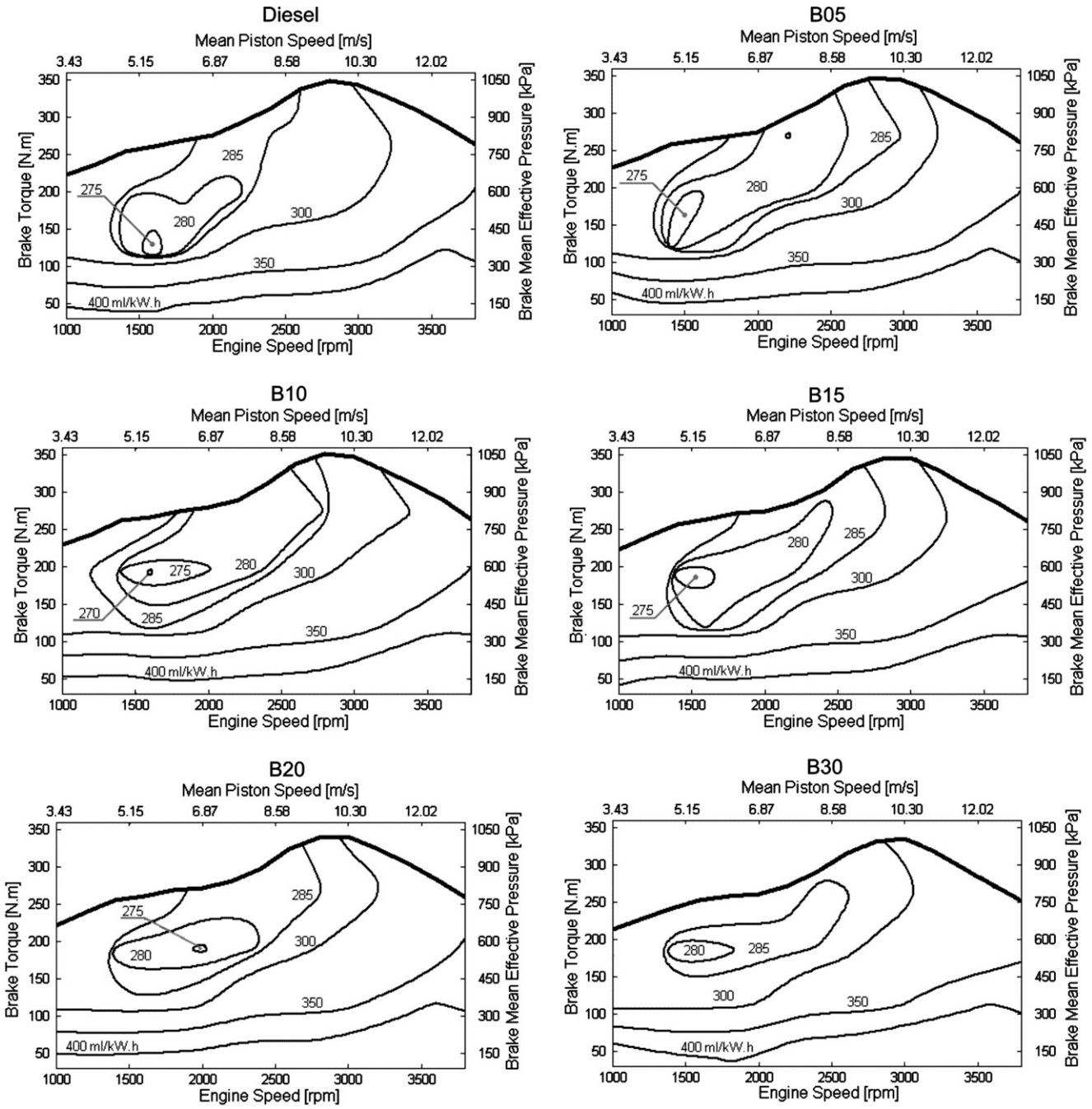

Fig. 8. Performance maps for diesel fuel/biodiesel blends.

biodiesel [42] and blends of other oxygenated compounds and diesel fuel [43–49]. The efficiency maps indicate greater modifications with biodiesel additions of up to 10% in volume, whereas the B20 blend presented a higher increase in efficiency in relation to the baseline fuel. An average increase of 4.16% was observed in the brake thermal efficiency for B20 blend and full load conditions. The causes of the thermal efficiency enhancements obtained with the use of biodiesel blends are investigated in the next section.

3.3. Fuel exergy allocation

In order to obtain some insight into the relative impact upon engine performance of each combustion modification caused by biodiesel properties, it is interesting to isolate the effects of the fuel burning acceleration verified with biodiesel blending from those imposed by mixture leaning and bulk temperature reduction. Obviously, it is not possible to obtain the input data necessary to accomplish this task with the exergy analysis model presented in the current work, which relies on experimental pressure diagrams where the above mentioned effects of biodiesel blending appear together.

For that reason, the consequences of the advance in heat release produced by the B20 fuel blend were addressed with exergy balances provenient from an engine simulation model [50,51]. This simulation model requires heat release curves represented by two Wiebe functions as input data, and also utilizes a single-zone working fluid representation. Two simulation conditions were employed with this purpose. The first one corresponds to a standard

diesel combustion at 2600 rpm and full load, and was considered here as the reference simulation case. The second simulation emulates the shorter combustion duration observed with biodiesel blending through a 2° advance of the Wiebe function correspondent to the mixing-controlled combustion, while maintaining the remaining input parameters of the reference case. The reference simulation was validated against experimental in-cylinder pressure data, as shown in Fig. 5a. From the very similar exergy balance results presented for the reference and advanced combustion simulations in Fig. 5b, it becomes evident that the combustion acceleration observed in the heat release analysis could not explain, by itself, the engine performance effects of biodiesel blending.

The exergy analysis results shown in the remaining of this section were obtained with experimental pressure data, which was processed by the model proposed in the current work. To reduce the uncertainties of calculated variables, the in-cylinder exergy balance analysis (see Equation (10)) involved full load engine operation and comparisons of the B20 blend, which showed greater deviations in efficiency in relation to the baseline fuel. In fact, variations in both fuel–air equivalence ratio and combustion temperature were found to govern the impact resulting from the addition of biodiesel on engine thermal efficiency. The combustion irreversibility rate is known to increase as the temperature of the working fluid decreases [52]. Due to the reduction in the fuel–air equivalence ratio and the decrease in the fuel heating value, it has been observed in Fig. 3c that biodiesel blends decrease mean in-cylinder temperatures, thus increasing combustion irreversibility. This expected trend is consistent with the results presented in Fig. 6, which shows that the use of the B20 blend led to an increase of the fraction of fuel exergy destroyed by irreversibilities (ΔI) in comparison with diesel fuel. On the other hand, the reductions of the fuel–air equivalence ratio and fuel C/H ratio achieved with biodiesel blending also increased the concentration of substances with low chemical exergies such as O_2 and H_2O, in detriment to the participation of substances with high chemical exergies such as CO_2, CO and H_2. Thus, the B20 blend showed a reduction in the loss of fuel exergy associated with the chemical exergy of end gases (ΔEx^{ch}). The lower bulk in-cylinder temperatures obtained with biodiesel blending diminish not only the heat transfer rate, but also the amount of thermomechanical exergy that is removed from the working fluid by heat transfer (see Equation (10)). Accordingly, the in-cylinder fuel exergy losses associated with heat transfer (ΔEx_Q) were also reduced with the B20 blend. For the engine and fuels studied here, these combined effects of biodiesel blending increased the amount of fuel exergy transferred through indicated work (ΔEx_W), thus augmenting the gross indicated thermal efficiency.

Full load operational regimes were also adopted for the in-cylinder exergy efficiency analysis. Fig. 7 presents gross indicated thermal efficiencies and exergy efficiencies obtained with diesel fuel, B10, B20 and B30 blends. On average, the combination of the above mentioned effects also enhanced the combustion exergy efficiency (η_b) by 0.42% for B10 blend, 0.75% for B20 blend and 0.19% for B30 blend in relation to diesel fuel. For the thermomechanical exergy transfer efficiency (η_{tm}), average increases of 1.15%, 3.24% and 2.82% were computed, respectively, for B10, B20 and B30 fuel blends. Hence, the following average variations were observed for the gross indicated thermal efficiency with relation to diesel fuel: B10 (+1.57%); B20 (+4.10%); B30 (+3.57%).

3.4. Sfc and brake torque

Performance maps obtained with baseline fuel, B05, B10, B15, B20 and B30 blends are shown in Fig. 8. In these maps, one can observe a reduction in *sfc* with biodiesel blending in concentrations up to 10% in volume, and an increase in *sfc* with further biodiesel addition. With respect to diesel fuel and in full load conditions, average reductions of 1.16%, 1.73%, 0.55% and 0.36% were observed in the *sfc* for B05, B10, B15 and B20 blends, respectively. Increases of 0.52% and 1.18% were observed, respectively, for B25 and B30 bends. For the engine and fuels utilized here, the engine *sfc* behavior is well represented by a balance between engine thermal efficiency elevation and fuel exergy reduction caused by biodiesel blending (see Equation (3)). Since engine thermal efficiency suffers greater improvements with biodiesel additions of up to 10% in volume while the fuel exergy is reduced in a quasi-linear way with the increase of the biodiesel concentration, this balance is favorable here to the B10 blend.

When analyzing the engine brake torque influence of biodiesel blending, the amount of fuel delivered to the engine has also to be taken into account (see Section 3.1 and Equation (2)). Concerning maximum brake torque and, accordingly, maximum brake power, the following average variations were observed for the analyzed blends with relation to diesel fuel: B05 (+0.40%); B10 (+1.15%); B15 (−0.37%); B20 (−1.67%); B25 (−2.83%); B30 (−4.76%).

4. Summary and conclusions

The performance effects of the addition of soybean oil ethyl ester were studied employing indicated and brake data obtained in steady-state experiments conduced with a turbocharged high speed diesel engine. Experimental data regarding overall fuel–air equivalence ratio, combustion reaction progress, exergy efficiencies, *sfc* and brake torque was reported for the engine operation with biodiesel blends of up to 30% in volume.

Biodiesel viscosity caused a reduction of the fuel mass flow rate as the concentration of biodiesel and the engine speed increased. Biodiesel's viscosity and oxygen content also contributed to a reduction of the local fuel–air equivalence ratio present in the fuel rich zones of the biodiesel spray combustion, accelerating the processes of mixture preparation and burning. In full load conditions, the crank angle interval required to a combustion reaction progress of 90% presented an average reduction of 1.81 for B10 blend, 1.87 for B20 blend and 1.97 for B30 blend with relation to diesel fuel.

For the engine and fuels utilized here, a balance between engine thermal efficiency elevation and fuel exergy reduction caused by biodiesel blending was found to govern the engine *sfc*. With respect to diesel fuel and in full load conditions, average reductions of 1.16%, 1.73%, 0.55% and 0.36% were observed in the *sfc* for B05, B10, B15 and B20 blends, respectively. Increases of 0.52% and 1.18% were observed, respectively, for B25 and B30 bends.

The impact of biodiesel blending in engine torque was governed by the above mentioned balance between engine efficiency elevation and fuel exergy reduction and, in addition, by the reduction in the amount of fuel delivered to the engine. Concerning full load brake torque and, accordingly, brake power, the following average variations were observed for the analyzed blends with relation to diesel fuel: B05 (+0.40%); B10 (+1.15%); B15 (−0.37%); B20 (−1.67%); B25 (−2.83%); B30 (−4.76%).

Acknowledgements

The authors acknowledge the Brazilian National Council for Scientific and Technological Development (CNPq) for financial support in this study under Grant Nos 479450/2007-2 and 552809/2007-1.

References

[1] Graboski MS, McCormick RL. Combustion of fat and vegetable oil derived fuels in diesel engines. Progress in Energy and Combustion Science 1998;24(2):125–64.

[2] Agarwal AK. Biofuels (alcohols and biodiesel) applications as fuels for internal combustion engines. Progress in Energy and Combustion Science 2007;33(3):233–71.
[3] Demirbas A. Progress and recent trends in biofuels. Progress in Energy and Combustion Science 2007;33(1):1–18.
[4] McCormick RL, Tennant CJ, Hayes RR, Black S, Ireland J, McDaniel T, et al. Regulated emissions from biodiesel tested in heavy-duty engines meeting 2004 emission standards. Society of Automotive Engineers; 2005. SAE Paper 2005-01-2200.
[5] United States Environmental Protection Agency. A comprehensive analysis of biodiesel impacts on exhaust emissions. Draft Technical Report. EPA420-P-02–001; 2002.
[6] Ali Y, Hanna MA, Leviticus LI. Emissions and power characteristics of diesel engines on methyl soyate and diesel fuel blends. Bioresource Technology 1995;52(2):185–95.
[7] Agarwal AK, Das LM. Biodiesel development and characterization for use as a fuel in compression ignition engines. Transactions of the ASME 2001;123:440–7.
[8] Al-Widyan MI, Tashtoush G, Abu-Qudais M. Utilization of ethyl ester of waste vegetable oils as fuel in diesel engines. Fuel Processing Technology 2001;76(2):91–103.
[9] Raheman H, Phadatare AG. Diesel engine emissions and performance from blends of karanja methyl ester and diesel. Biomass and Bioenergy 2004;27(4):393–7.
[10] Ramadhas AS, Muraleedharan C, Jayaraj S. Performance and emission evaluation of a diesel engine fueled with methyl esters of rubber seed oil. Renewable Energy 2005;30(12):1789–800.
[11] Labeckas G, Slavinskas S. The effect of rapeseed oil methyl ester on direct injection diesel engine performance and exhaust emissions. Energy Conversion and Management 2006;47(13):1954–67.
[12] Lin YC, Lee WJ, Hou HC. PAH emissions and energy efficiency of palm-biodiesel blends fueled on diesel generator. Atmospheric Environment 2006;40(21):3930–40.
[13] Raheman H, Ghadge SV. Performance of diesel engine with biodiesel at varying compression ratio and ignition timing. Fuel 2008;87(12):2659–66.
[14] Bueno AV, Velásquez JA, Milanez LF. Effect of soybean oil ethyl ester/diesel fuel blend on engine efficiency. International Journal of Vehicle Design 2009;50(1):229–47.
[15] Godiganurb S, Murthy CHS, Reddy RP. 6BTA 5.9 G2–G1 Cummins engine performance and emission tests using methyl ester mahua (*Madhuca indica*) oil/diesel blends. Renewable Energy 2009;34(10):2172–7.
[16] Monyem A, Van Gerpen JH. The effect of biodiesel oxidation on engine performance and emissions. Biomass and Bioenergy 2001;20(4):317–25.
[17] Canakci M. Performance and emissions characteristics of biodiesel from soybean oil. Proceedings of the institution of mechanical engineers, part D. Journal of Automobile Engineering 2005;219(7):915–22.
[18] Rakopoulos CD, Antonopoulos KA, Rakopoulos DC, Hountalas DT, Giakoumis EG. Comparative performance and emissions study of a direct injection diesel engine using blends of diesel fuel with vegetable oils or biodiesels of various origins. Energy Conversion and Management 2006;47(18):3272–87.
[19] Rakopoulos CD, Rakopoulos DC, Hountalas DT, Giakoumis EG, Andritsakis EC. Performance and emissions of bus engine using blends of diesel fuel with biodiesel of sunflower or cottonseed oils derived from Greek feedstock. Fuel 2008;87(2):147–57.
[20] Tsolakis A, Megaritis A, Wyszynski ML, Theinnoi K. Engine performance and emissions of a diesel engine operating on diesel-RME (rapeseed methyl ester) blends with EGR (exhaust gas recirculation). Energy 2007;32(11):2072–80.
[21] Lin YC, Lee WJ, Wu TS, Wang CT. Comparison of PAH and regulated harmful matter emissions from biodiesel blends and paraffinic fuel blends on engine accumulated mileage test. Fuel 2006;85(17):2516–23.
[22] Baiju B, Naik MK, Das LM. A comparative evaluation of compression ignition engine characteristics using methyl and ethyl esters of Karanja oil. Renewable Energy 2009;34(6):1616–21.
[23] Kaplan C, Arslan R, Sürmen A. Performance characteristics of sunflower methyl esters as biodiesel. Energy Sources 2006;28(8):751–5.
[24] Choi CY, Reitz RD. An experimental study on the effects of oxygenate fuel blends and multiple injection strategies on DI diesel engine emissions. Fuel 1999;78(11):1303–27.
[25] Serdari A, Fragioudakis K, Kalligeros S, Stournas S, Lois E. Impact of using biodiesels of different origin and additives on the performance of a stationary diesel engine. Journal of Engineering for Gas Turbines and Power 2000;122(4):624–31.
[26] Alam M, Song J, Acharya R, Boehman A, Miller K. Combustion and emissions performance of low sulfur, ultra low sulfur and biodiesel blends in a DI diesel engine. Society of Automotive Engineers; 2004. SAE Paper 2004-01-3024.
[27] Carraretto C, Macor A, Mirandola A, Stoppato A, Tonon S. Biodiesel as alternative fuel: experimental analysis and energetic evaluations. Energy 2004;29(12):2195–211.
[28] Aydin H, Bayindir H. Performance and emission analysis of cottonseed oil methyl ester in a diesel engine. Renewable Energy 2010;35(3):588–92.
[29] Randolph AL. Methods of processing cylinder-pressure transducer signals to maximize data accuracy. Society of Automotive Engineers; 1990. SAE Paper 900170.
[30] Bueno AV, Velásquez JA, Milanez LF. A new engine indicating measurement procedure for combustion heat release analysis. Applied Thermal Engineering 2009;29(14):1657–75.
[31] Krieger RB, Borman GL. The computation of apparent heat release for internal combustion engines. American Society of Mechanical Engineers; 1966. ASME paper 66-WA/DGP-4.
[32] Olikara C, Borman GL. A computer program for calculating properties of equilibrium combustion products with some applications to I.C. engines. Society of Automotive Engineers; 1975. SAE Paper 750468.
[33] Annand WJD, Ma TH. Instantaneous heat transfer rates to the cylinder head surface of a small compression-ignition engine. Proceedings of the institution of mechanical engineers, part D. Journal of Automobile Engineering 1971;185:976–87.
[34] Shapiro HN, Van Gerpen JH. Two zone combustion models for second law analysis of internal combustion engines. Society of Automotive Engineers; 1989. SAE Paper 890823.
[35] Stepanov VS. Chemical energies and exergies of fuels. Energy 1995;20(3):235–42.
[36] Van Gerpen JH, Shapiro HN. Second law analysis of diesel engine combustion. ASME–AESD Analysis and Design of Advanced Energy Systems: Computer Aided Analysis and Design 1987;3(3):53–65.
[37] Chang C, Farrell P. A study on the effects of fuel viscosity and nozzle geometry on high injection pressure diesel spray characteristics. Society of Automotive Engineers; 1997. SAE Paper 970353.
[38] Bang SH, Lee CS. Fuel injection characteristics and spray behavior of DME blended with methyl ester derived from soybean oil. Fuel 2010;89(3):797–800.
[39] Fang T, Lin YC, Foong TM, Cf Lee. Biodiesel combustion in an optical HSDI diesel engine under low load premixed combustion conditions. Fuel 2009;88(11):2154–62.
[40] Rakopoulos CD, Antonopoulos KA, Rakopoulos DC. Development and application of multi-zone model for combustion and pollutants formation in direct injection diesel engine running with vegetable oil or its bio-diesel. Energy Conversion and Management 2007;48(7):1881–901.
[41] Chmela FG, Orthamber GC. Rate of heat release and its prediction for direct injection diesel engines based on purely mixing controlled combustion. Society of Automotive Engineers; 1999. SAE Paper 1999-01-0186.
[42] Tormos B, Novella R, García A, Gargar K. Comprehensive study of biodiesel fuel for HSDI engines in conventional and low temperature combustion conditions. Renewable Energy 2010;35(2):368–78.
[43] Miyamoto N, Ogawa H, Nurun N, Obata K, Arima T. Smokeless, low NO_x, high thermal efficiency, and low noise diesel combustion with oxygenated agents as main fuel. Society of Automotive Engineers; 1998. SAE Paper 980506.
[44] Miles PC. Combustion of an ethanol/diesel fuel blend in an HSDI diesel engine. In: Payri F, Whitelaw JHW, editors. Thermal and fluid-Dynamic processes in diesel engines. New York: Springer. p. 107–32.
[45] Yanfeng G, Shenghu L, Hejun G, Tiegang H, Longbao Z. A new diesel oxygenate additive and its effects on engine combustion and emissions. Applied Thermal Engineering 2007;27(1):202–7.
[46] Rakopoulos CD, Antonopoulos KA, Rakopoulos DC. Experimental heat release analysis and emissions of a HSDI diesel engine fueled with ethanol–diesel fuel blends. Energy 2007;32(10):1791–808.
[47] Rakopoulos DC, Rakopoulos CD, Kyritsis DC, Papagiannakis RG, Giakoumis EG. Experimental-stochastic investigation of the combustion cyclic variability in HSDI diesel engine using ethanol–diesel fuel blends. Fuel 2008;87(8):1478–91.
[48] Xingcai L, Jianguang Y, Wugao Z, Zhen H. 'Effect of cetane number improver on heat release rate and emissions of high speed diesel engine fuelled with ethanol–diesel blend fuel'. Fuel 2004;83:2013–20.
[49] Xingcai L, Zhen H, Wugao Z, Degang L. 'The influence of ethanol additives on the performance and combustion characteristics of diesel engines'. Combustion Science and Technology 2004;176:1309–29.
[50] Velásquez JA, Milanez LF. Analysis of the irreversibilities in diesel engines. Society of Automotive Engineers; 1994. SAE Paper 940673.
[51] Velásquez JA, Milanez LF. A computational model for simulation of processes in diesel engines. Society of Automotive Engineers; 1995. SAE Paper 952304.
[52] Caton JA. On the destruction of availability (exergy) due to combustion process – with specific application to internal-combustion engines. Energy 2000;25(11):1097–117.